Title

SAFETY AND TOLERABILITY OF MRI-GUIDED INFUSION OF AAV2-hAADC INTO THE MID-BRAIN OF NON-HUMAN PRIMATE.

Authors

Samaranch, Lluis

Hadaczek, Piotr

Ciesielska, Agnieszka

et al.

Publication Date

2014-10-15

DOI

10.1038/mtm.2014.49

Peer reviewed

Citation: Molecular Therapy — Methods & Clinical Development (2014) **3,** 14049; doi:10.1038/mtm.2014.49

www.nature.com/mtm

ARTICLE

Safety and tolerability of MRI-guided infusion of AAV2-hAADC into the mid-brain of nonhuman primate

Waldy San Sebastian[1], Adrian P Kells[1], John Bringas[1], Lluis Samaranch[1], Piotr Hadaczek[1], Agnieszka Ciesielska[1], Michael J Macayan[1], Phillip J Pivirotto[1], John Forsayeth[1], Sheryl Osborne[2], J Fraser Wright[3,4], Foad Green[1], Gregory Heller[1] and Krystof S Bankiewicz[1]

Aromatic L-amino acid decarboxylase (AADC) deficiency is a rare, autosomal-recessive neurological disorder caused by mutations in the *DDC* gene that leads to an inability to synthesize catecholamines and serotonin. As a result, patients suffer compromised development, particularly in motor function. A recent gene replacement clinical trial explored putaminal delivery of recombinant adeno-associated virus serotype 2 vector encoding human AADC (AAV2-hAADC) in AADC-deficient children. Unfortunately, patients presented only modest amelioration of motor symptoms, which authors acknowledged could be due to insufficient transduction of putamen. We hypothesize that, with the development of a highly accurate MRI-guided cannula placement technology, a more effective approach might be to target the affected mid-brain neurons directly. Transduction of AADC-deficient dopaminergic neurons in the substantia nigra and ventral tegmental area with locally infused AAV2-hAADC would be expected to lead to restoration of normal dopamine levels in affected children. The objective of this study was to assess the long-term safety and tolerability of bilateral AAV2-hAADC MRI-guided pressurized infusion into the mid-brain of nonhuman primates. Animals received either vehicle, low or high AAV2-hAADC vector dose and were euthanized 1, 3, or 9 months after surgery. Our data indicate that effective mid-brain transduction was achieved without untoward effects.

Molecular Therapy — Methods & Clinical Development (2014) **3**, 14049; doi:10.1038/mtm.2014.49; published online 15 October 2014

INTRODUCTION

Aromatic L-amino acid decarboxylase (AADC) deficiency is a rare recessive genetic disorder in which mutations in the *DDC* gene (DOPA decarboxylase, NG_008742) lead to deficient synthesis of catecholamines (dopamine, norepinephrine, epinephrine) and serotonin. Over 100 cases with more than 30 different mutations in the AADC gene (http://www.biopku.org) have been identified worldwide[1,2] since the original description of the disorder in 1990.[3] Affected children suffer chronic and severe motor, cognitive, and behavioral disability. The most prominent neurological symptoms are motor: hypokinesia, hypotonia, oculogyric crises, involuntary movements, and motor developmental delay.[4] Because of the lack of AADC, which catalyzes conversion of levodopa (L-DOPA) to dopamine, motor symptoms do not respond to therapy with L-DOPA, in contrast to the positive response observed in Parkinson's disease (PD) and some other inborn errors of dopamine metabolism.[5,6] Most patients with AADC deficiency obtain little if any symptomatic benefit from currently available medical therapies.[4]

In recent years, use of a viral vector, adeno-associated virus type 2 (AAV2), encoding the cDNA of human *DDC* gene (hAADC), has been developed for the treatment of PD. Initial studies have demonstrated that the gene can be safely delivered to the striatum in human subjects via targeted infusion in adult PD patients.[7,8] More recently, a phase 1 clinical study was conducted in children with AADC deficiency.[9] These pediatric patients received a bilateral AAV2-hAADC infusion into the putamen that resulted in moderate motor performance improvement and an increase in 6-[^{18}F]fluoro-DOPA uptake, a tracer for AADC, in all subjects. The trial investigators acknowledged that the vector might have only partially covered the putamen accounting for mild motor improvement in patients. Perhaps a more important issue, however, is that AAV2 does not undergo retrograde axonal transport in the brain and putaminally infused vector would not be expected to transduce affected catecholaminergic neurons with any appreciable efficiency.[10,11] Moreover, anterograde transport of AAV2 and gene product after putaminal infusion results in AADC expression in many nontargeted nuclei such as globus pallidus, subthalamic nucleus, and substantia nigra pars reticulata (SNpr).[11,12] Unlike in PD, where there is extensive degeneration of dopaminergic nigrostriatal neurons, dopamine transporter (TRODAT) imaging reveals that the nigrostriatal pathway is largely unaffected in AADC deficiency.[1] For all these reasons, we believe that vector should be infused directly into affected nuclei to transduce the AADC-deficient catecholaminergic neurons. This approach requires a level of accuracy of cannula placement that,

The first two authors contributed equally to this work.

[1]Department of Neurological Surgery, University of California San Francisco, San Francisco, California, USA; [2]Consultant; [3]Center for Cellular and Molecular Therapeutics, Children's Hospital of Philadelphia, Philadelphia, Pennsylvania, USA; [4]Department of Pathology and Laboratory Medicine, University of Pennsylvania Perelman School of Medicine, Philadelphia, Pennsylvania, USA Correspondence: Krystof S Bankiewicz, Department of Neurological Surgery, University of California San Francisco, 1855 Folsom Street, MCB 226, San Francisco, CA 94103-0555, USA. E-mail: Krystof.Bankiewicz@ucsf.edu

Received 15 May 2014; accepted 31 August 2014

until recently, was challenging. Accordingly, we have developed an MRI-guided infusion platform in nonhuman primates (NHP) to achieve improved control of infusate delivery and visualization of therapeutic distribution in the brain,[13–15] and this approach has now been integrated into two phase 1 clinical trials in PD for AAV2-glial cell line-derived neurotrophic factor (NCT01621581) and AAV2-hAADC (NCT01973543).

In this article, we report the safety and tolerability of bilateral AAV2-hAADC real-time image-guided infusion into the mid-brain of adult NHP for up to 9 months after surgery. Our data indicate that this approach results in broad coverage of targeted areas (substantia nigra pars compacta (SNpc) and ventral tegmental area (VTA)) and widespread AADC protein distribution in the striatum can be achieved by dopaminergic neurons without inducing any adverse effects. This study supports testing mid-brain administration of AAV2-hAADC in a clinical study as a possible gene therapy for AADC-deficient patients.

RESULTS

Two experiments were performed in this study (Table 1): (i) an initial pilot study to examine vector distribution, dose-ranging and initial safety after delivery into the mid-brain (N = 2) and (ii) an Investigational New Drug (IND)-enabling study to assess long-term safety and toxicology of AAV2-hAADC administration to mid-brain (Control group (vehicle, N = 4), AAV2-hAADC low-dose group (N = 6) and high-dose group (N = 6)).

Infusion performance

In both studies, AAV2-hAADC (N = 14) or vehicle (N = 4) was used to infuse the right and left SNpc and VTA (total of 36 cannula insertions). Up to 46 µl of the infusate per hemisphere was infused bilaterally (30 µl per side in the toxicology study). Gadolinium-enhanced magnetic resonance images (MRI) from each infusion confirmed that positioning of each cannula was accurate and infusate covered the target area (Figure 1). All of the 36 infusions were well contained in the target structure with slight reflux seen along the cannula tract in only two cases (Figure 1: V002458, left side; V002254, right side). Three-dimensional reconstructions of the infusate distribution generated from gadolinium signal on MR images showed that both placement and distribution of infusate were very consistent throughout all the animals (Supplementary Figure S1). As well, the ratio (Vd/Vi) between volume of distribution (Vd) and volume of infusion (Vi) was calculated for each delivery and data were consistent across infusions in both studies. Vd was approximately twofold larger than the Vi (pilot study: 2.23 ± 0.24; toxicology study: 2.18 ± 0.52; Figure 1 and Supplementary Table S1). No MRI-visible hemorrhages occurred during cannula placement and no adverse events occurred during infusion or subsequently.

Intervention-related pathology

All animals (N = 18) tolerated the AAV dosing procedure with no treatment-related adverse events over a 9-month evaluation period. Hematology, clinical pathology, body-weight, general activity and behavior remained unchanged. A detailed neurobehavioral assessment was performed at baseline and prior to

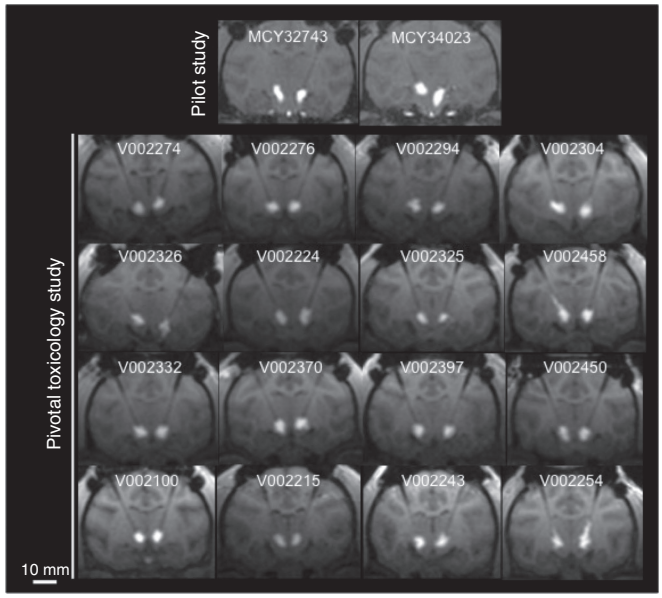

Study	Infusion volume (per site)	Vd/Vi
Pilot	26–46 µl	2.23 ± 0.24
GLP toxicology	30 µl	2.18 ± 0.52

Figure 1 Reproducibility of magnetic resonance (MR) image-guided infusion of AAV2-hAADC into the primate mid-brain. Top panel shows representative coronal MR images of AAV2-hAADC after pressure-driven delivery in each animal. Please note there was slight reflux in only 2 out of 36 infusion performed (V002458 and V002254). Summary table below presents diffusion volume/infusion volume ratio (Vd/Vi, mean ± SD) for pilot and toxicology groups.

Table 1 Dosing groups and necropsy schedule

Pilot study					
Group	*Vector conc. (vg/ml)*	*Vector dose (vg)*	*Survival time*		
AAV2-hAADC high dose	8.3×10^{12}	5.0×10^{11}-6.0×10^{11}	1 month (n = 2, female)		
Pivotal toxicology study					
			Survival time groups (male + female)		
Group	*Vector conc. (vg/ml)*	*Vector dose (vg)*	*1 month* (n = *5)*	*3 months* (n = *5)*	*9 months* (n = *6)*
Control	0	0	1 male	1 male	2(1 + 1)
AAV2-hAADC low dose	8.3×10^{11}	5.0×10^{10}	2(1 + 1)	2(1 + 1)	2(1 + 1)
AAV2-hAADC high dose	8.3×10^{12}	5.0×10^{11}	2(1 + 1)	2(1 + 1)	2(1 + 1)

Conc., concentration; vg, vector genome.

euthanasia which evaluated cranial nerves, menace, pupil size, bite reflex and strength, strabismus, facial symmetry, cochlear response, head tilt, nystagmus, gait, posture, muscle tone, placing and proprioception. No neurobehavioral abnormalities were observed during the study. Also, gross examination at necropsy showed no remarkable findings related to the experimental treatment. In order to rule out that the absence of adverse effects was due to a nonfunctional vector, we confirmed AAV2-hAADC performance *in vitro*. Cell-based assay demonstrated increased L-DOPA conversion to dopamine in AAV2-hAADC transduced cells compared to nontransduced ones and increased dopamine production with increasing multiplicity of infection (MOI, Supplementary Figure S2).

Hematoxylin and eosin (H&E) staining of the infusion site in pilot animals demonstrated some gliosis located only around the cannula tract (Figure 2). Similarly, an independent histopathology report on toxicological study animals revealed vacuolated macrophages and gliosis attributable to the infusion procedure itself, because it was present in both control and AAV2-hAADC-treated groups (low- or high-dose) either 1, 3, or 9 months after infusion. Gliosis was less commonly observed at 9 months than at 1 or 3 months and was considered evidence of partial resolution of the damage associated with the infusion procedure. Also, independent histopathological assessment in the toxicology study showed the presence of perivascular mononuclear cell infiltrates only in animals receiving AAV2-hAADC infusion at either low- or high-dose. Nevertheless, they were

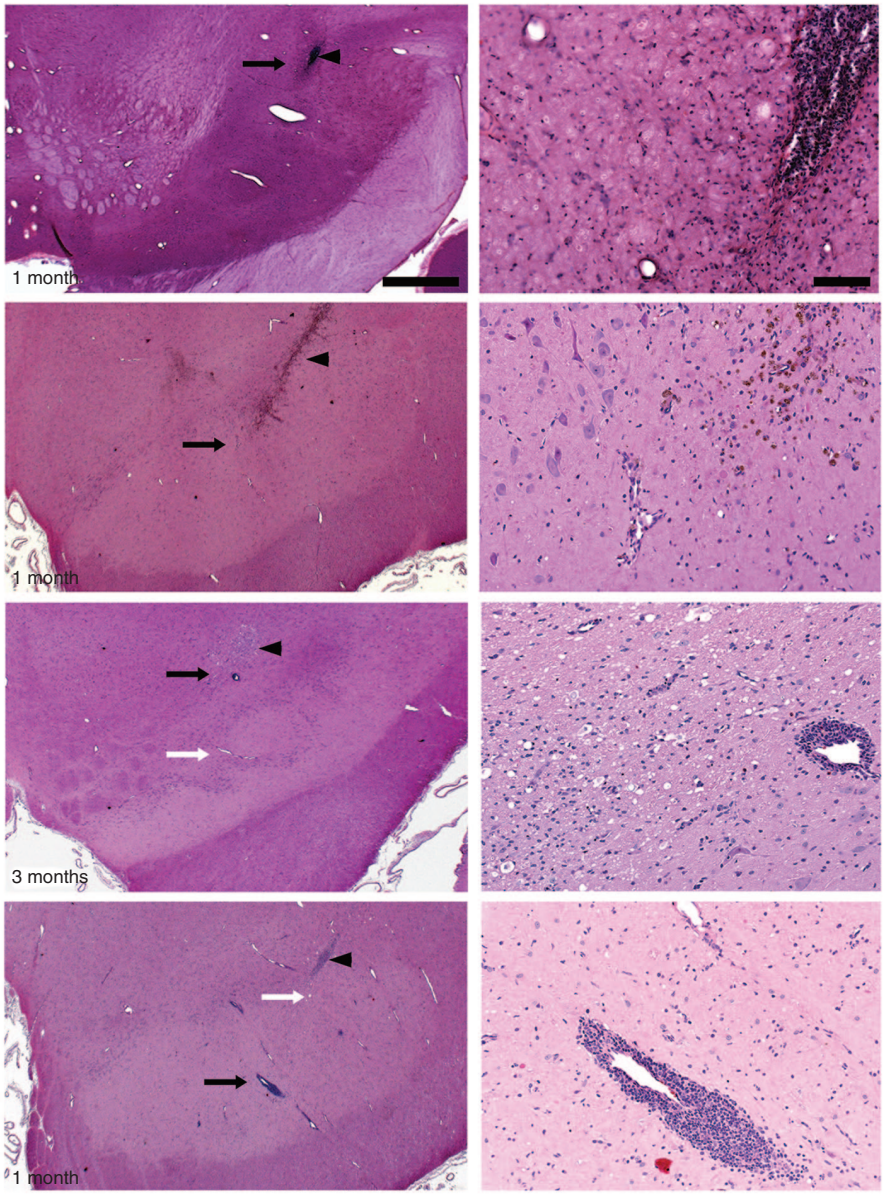

Figure 2 Surgery and vector-related histological findings. Independent evaluation of hematoxylin and eosin (H&E) staining of coronal sections containing the cannula tract revealed normal gliosis related to cannula insertion in all experimental groups (arrowheads). Higher magnification images (right column) were taken close to the cannula tip (black arrows in left column). H&E staining also showed perivascular cellular infiltrates in AAV2-hAADC-treated, but not PBS-treated, animals regardless of survival time. Although incidence and severity of perivascular cuffs was increased with AAV2-hAADC vector dose, these were not considered adverse. Note that there were also many vessels with no perivascular cuffing close to the infusion site (white arrows in left column) and that perivascular cellular infiltrates were not present in the pilot AAV2-hAADC animal. Scale bars: left column: 1 cm; right column: 100 µm.

not considered adverse since animals displayed no symptomatology associated with it. In addition, there were no pathological findings related to infusion with the test article in either the spinal cord or major organ tissues.

AADC transgene expression in the brain

Neurons in the SNpc and VTA express endogenous AADC that made difficult to distinguish transduced neurons from those not transduced in these nuclei. Nevertheless, the distribution and intensity of immunohistochemical AADC staining in the mid-brain of AAV2-hAADC-treated animals clearly showed increased AADC expression within the targeted area when compared to mid-brain staining in control animals (Figure 3a (pilot) and 3B (pivotal toxicology)). In some of the animals, transgenic hAADC signal was noted in the lateral SNpr, normally devoid of AADC, both in double chromogenic (Figure 3) and double immunofluorescent sections (Supplementary Figure S3). Histological sections in some of the animals revealed the cannula tract, thereby confirming optimal placement of the cannula and matching observed MRI tracer (Figure 2) in VTA and medial-lateral SNpc.

AADC immunohistochemical staining was semi-quantitatively analyzed by observers blind to the treatment groups. Coronal brain sections containing either the precommissural, commissural, postcommissural striatum, and other basal ganglia nuclei were included in the analysis of the striatal and off-target AADC transgene expression. Transduction of SNpc and VTA neurons resulted in the expression of hAADC in these neurons and the filling of neuronal cytoplasm with the hAADC protein. Thus, since those neurons project axons to the striatum, we detected increased AADC protein in caudate nucleus, putamen and nucleus accumbens in AAV2-hAADC animals compared to control group. Transgenic AADC expression in the striatum was robust, widely distributed and restricted to neuronal fibers (Figure 4) in both AAV2-hAADC-treated groups, regardless of vector dose or survival time. Four out of six animals in both low- and high-dose groups exhibited prominent AADC-immunoreactive (ir) fibers whereas the other two animals in each group presented fewer fibers, mainly in the most anterior sections examined

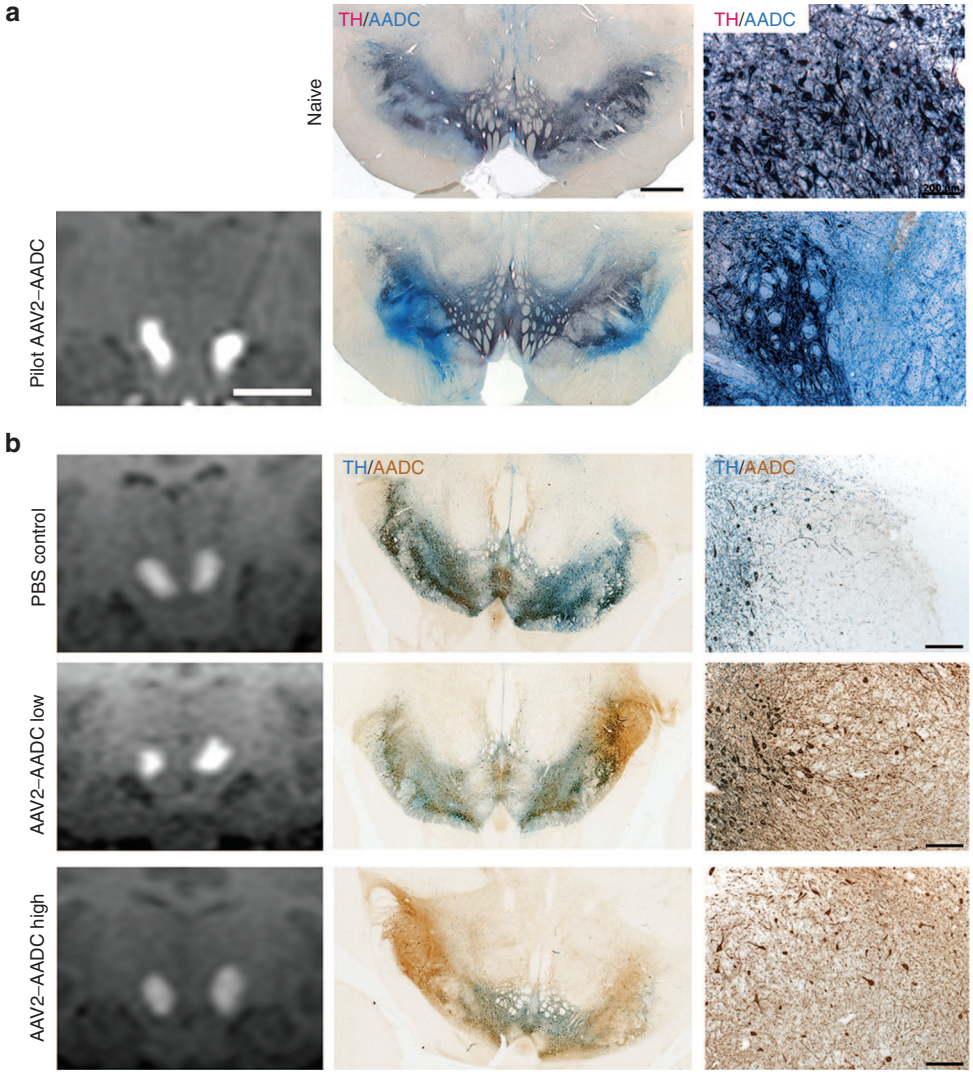

Figure 3 AADC expression in the mid-brain of (**a**) pilot and (**b**) toxicology study animals. AADC staining of mid-brain revealed good correlation between infusate (gadolinium) signal in MRI and AAV2-hAADC expression (left and middle columns). AADC signal (brown) in SNpc and VTA that colocalized with endogenous tyrosine hydroxylase signal (blue, middle column). Although transgenic AADC in these nuclei was indistinguishable from endogenous AADC, AAV2-hAADC gene product was easily visible in SNpr when compared to naïve animal images. Higher magnification images show transgenic AADC staining in cells and fibers (right column). Scale bars: Left and middle columns: 1 cm; right column: 200 µm.

(Supplementary Table S2). As expected, animals in the control group displayed no evidence of transgenic hAADC, with AADC-ir restricted to light staining consistent with endogenous expression (Figure 4 and Table 2). This was further confirmed with double immunofluorescent staining against TH and AADC in tissue sections containing striatum, where fluorescent intensity of AADC fibers was stronger in AAV2-hAADC-treated animals, regardless of vector dose (Supplementary Figure S3). With respect to nucleus accumbens, only two animals presented a few intense AADC-ir fibers in the core but none in the shell region. There was no significant effect of survival time among AAV2-hAADC or control groups, nor was there a significant vector dose effect on AAV2-hAADC-treated groups.

Distribution of AADC-ir fibers in the striata also matched the cannula positioning in the mid-brain (*i.e.*, slightly anterior positioning of cannula in the mid-brain yielded anterior distribution of fibers in the striatum), explaining the gradient of AADC-ir fibers detected in some of the AAV2-hAADC-treated animals. There were no medium spiny neurons stained for AADC within any of the striata analyzed in either the low- or high-dose groups, indicating that all of the AADC-positive fibers were nigrostriatal projections. Accordingly, double immunofluorescent staining of AADC and DARPP32, a striatal medium spiny neuron marker, showed no DARPP32-ir neurons that coexpressed AADC in the striatum of either group (Supplementary Figure S4).

Analysis of off-target hAADC expression was performed throughout brain structures including other components of the basal ganglia (*i.e.*, globus pallidus, subthalamic nucleus), hypothalamus, thalamus, brainstem, and spinal cord (Table 3). Most of the off-target expression of the transgene was found in the region dorsal to SN (*i.e.*, red nucleus) and was mostly fibers, although some animals presented a few hAADC-ir neurons in the red nucleus. Sparse fibers and neuronal cells expressed hAADC outside the infusion area and the endogenously expressing structures, but they were restricted to areas proximal to the cannula tracts (Supplementary Tables S3 and S4). Accordingly, some AADC-ir fibers and neuronal cell bodies were visible in the subthalamic nucleus and the thalamus for some of the animals. Many animals exhibited several thick hAADC-ir fibers traversing the corona radiata and the internal capsule, and arising from cortical neurons close to the cannula entry point. Four out of 16 animals contained several hAADC-expressing fibers in the spinal cord that corresponded to projections from either the cortex or the red nucleus. Overall, hAADC transgene expression was restricted to the infusion site and expression outside the target structures (SN and VTA) was limited to tissue around the cannula tracts.

Monoamines and their metabolites levels in CSF

In the toxicological study, dopamine, 3,4-dihydroxyphenylacetic acid (DOPAC), homovanillic acid (HVA), serotonin and 5-hydroxyindoleacetic acid (5-HIAA) were measured in cerebrospinal fluid (CSF) at baseline and at necropsy. Dopamine, DOPAC and serotonin levels in CSF were below the limit of quantification, but HVA and 5-HIAA could be detected in all animals at baseline (Supplementary Table S5). Two animals in the AAV2-hAADC low-dose group had detectable dopamine levels at necropsy (1 and 3 months after vector delivery, respectively). One also had quantifiable levels of serotonin and DOPAC but no change in HVA and 5-HIAA levels. No animals in the AAV2-hAADC high-dose group had detectable levels of either dopamine or serotonin before or after AADC gene transfer nor did they show changes in monoamine metabolites after vector delivery at any time-point (1, 3, or 9 months after vector delivery). Overall, no significant changes in dopamine, serotonin or their metabolite levels were found in the CSF after AAV2-hAADC gene transfer.

Vector distribution, AADC protein levels and antibody production

AAV2-hAADC vector distribution. Detection of AAV2-hAADC DNA in serum and CSF samples was performed by real-time Q-PCR. The presence of vector sequences in the serum was determined in serum samples collected 4 hours after AAV2-hAADC delivery, and in both serum and CSF samples immediately prior to necropsy.

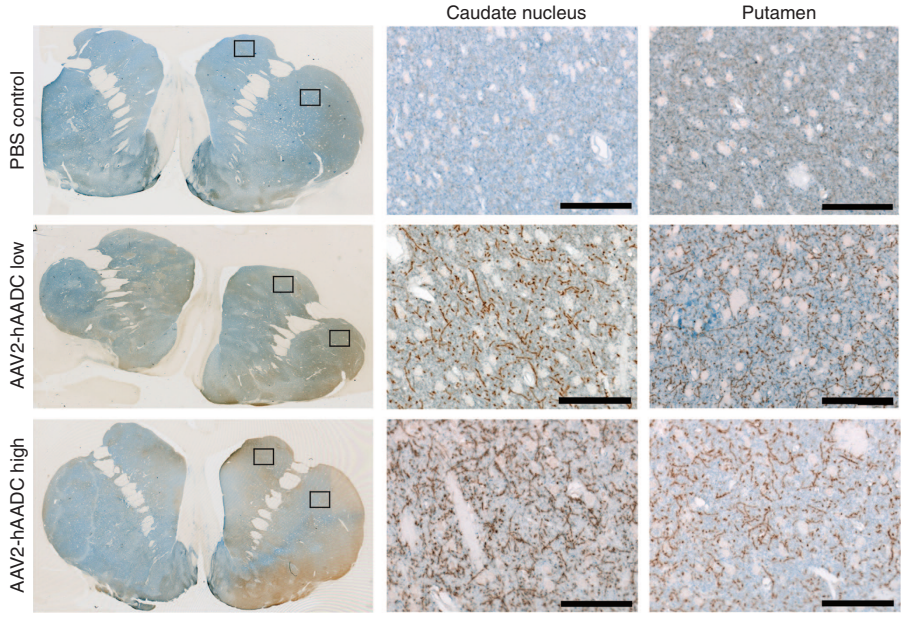

Figure 4 Axonal transport of AADC protein through the nigrostriatal pathway. Double immunohistochemical staining for TH (blue) and AADC (brown) in the striatum demonstrated the presence of the transgenic AADC in nigrostriatal terminals that widely covered both caudate and putamen nuclei. High-magnification images show the intensity of AADC staining in transduced fibers in AAV2-hAADC-treated animals compared to endogenous signal in PBS control group. Black squares indicate the area shown in higher magnification images. Notice the similar fiber density for both low and high AAV2-hAADC doses. Scale bar: 100 µm.

Table 2 Transgenic AADC-positive fibers in striatum (caudate nucleus and putamen) and nucleus accumbens

NHP ID (survival)	*Caudate nucleus*	*Putamen*	*Nucleus accumbens*[a]
Control group			
V002326 (1 month)	–	–	–
V002215 (1 month)	–	–	–
V002397 (3 months)	–	–	–
V002458 (9 months)	–	–	–
AAV2-hAADC low dose group			
V002243 (1 month)	+++	+++	–
V002274 (1 month)	++/+++	++/+++	–
V002254 (3 months)	+	+	–
V002294 (3 months)	++/+++	++/+++	+
V002100 (9 months)	+++	++	++
V002276 (9 months)	+++	++	
AAV2-hAADC high dose group			
V002332 (1 month)	+++	++	–
V002370 (1 month)	++/+++	++/+++	–
V002224 (3 months)	+++	++/+++	+
V002304 (3 months)	++/+++	++	–
V002325 (9 months)	++	+/++	–
V002450 (9 months)	+++	+++	+

AADC-ir fiber staining rating: –, absent (endogenous AADC staining); +, low intensity/sparse fiber staining; ++, intermediate intensity/many positive fibers; +++, high intensity/dense fiber staining.
[a]AADC-positive fibers were found only in nucleus accumbens core.

Vector DNA copies in serum of control and AAV2-hAADC low-dose groups were below the limit of detection (10 copies/ml) either 4 hours after vector delivery or at necropsy. In the high-dose group, four animals had AAV2-hAADC DNA in serum 4 hours after surgery. Three of them had no detectable DNA at necropsy and the fourth a dramatically lower copy number (sevenfold less). One animal that did not exhibit vector DNA in blood serum 4 hours after delivery did show DNA levels above the assay sensitivity threshold at necropsy (Supplementary Table S6). No AAV2-hAADC DNA was detected in CSF samples in any of the groups at necropsy. These results indicate some systemic exposure during or immediately after infusion of AAV2-hAADC to the mid-brain.

AADC protein levels in serum and CSF. Quantification of AADC levels in serum and CSF samples was performed by sandwich ELISA assay. Serum AADC levels at baseline (prior to AAV2-hAADC delivery) ranged considerably between animals with 9 out of 16 animals showing AADC levels below the detection limit and 2 animals with more than 2.5 ng/ml (Supplementary Table S7). Nine months after AAV2-hAADC delivery, serum and CSF AADC protein level was generally unchanged from baseline, except for two animals in the high-dose group and one animal in the low-dose group with 7-fold, 2.4-fold, and 2.4-fold increases, respectively. However, only one animal had detectable serum and CSF AADC protein 3 months after receiving a high dose of AAV2-hAADC and none at baseline. Overall, serum and CSF levels of AADC were generally very low after AAV2-hAADC delivery.

Table 3 Off-target expression of transgenic hAADC protein

Brain structure	*AAV2-hAADC low dose*	*AAV2-hAADC high dose*
Globus pallidus	F	F
Thalamus	F/C[a]	F/C[a]
Medial forebrain bundle	–	F
Subthalamic nucleus	F/C[a]	F/C[a]
Substantia nigra pars reticulata	F	F
Red nucleus	F/C	F/C
Spinal cord	–	F
Other	F	F
	Corona radiata/IC area dorsal to SN	Corona radiata/IC area dorsal to SN

C, cells; F, fibers; IC, internal capsule.
[a]Surrounding cannula tract.

Neutralizing anti-AAV2 and anti-hAADC antibodies. Antibody titers for neutralizing antibodies against AAV2 and antibodies against hAADC were measured in serum samples collected prior to surgery (baseline) and at necropsy (1, 3, and 9 months after vector delivery). Anti-AAV2 antibody titers were predominantly ≤1:25 before brain delivery of either vehicle or AAV2-hAADC for all the animals, except for a single animal in the control group whose titer was 1:50 (Supplementary Table S8). At necropsy, anti-AAV2 antibody titers in control and AAV2-hAADC low-dose groups remained ≤1:25. However, animals in AAV2-hAADC high-dose group presented titers between 1:50 and 1:1,600, regardless of survival time. Neutralizing AAV2 antibodies are not anticipated to cause any adverse effects but could affect subsequent AAV-mediated gene transfer if repeated dosing with the same serotype were to be considered.

Regarding anti-hAADC antibodies, all animals showed antibodies against AADC protein in baseline samples, suggesting a natural presence of a reactive antibody in naïve animals (endogenous-load, Supplementary Figure S5). Measurements of antibody titers against AADC protein at the time of necropsy showed no substantial increase when compared to baseline levels in either the controls or AAV2-hAADC-treated animals, regardless of the dose (Supplementary Figure S5). This result (ratio: ~1.0) indicates that parenchymal delivery of AAV2-hAADC did not induce anti-AADC antibodies.

DISCUSSION

The purpose of this study was to investigate the safety and tolerability of a single-dose of AAV2-hAADC delivered into the mid-brain of NHP as a possible gene therapy for AADC deficiency. Previous studies on the striatal administration of AAV2-hAADC in NHP[15–19] and PD patients,[7,8,20,21] support the use of this vector for the treatment of AADC deficiency. A phase 1 study was conducted in Taiwan where four AADC deficiency patients that received a striatal AAV2-hAADC infusion showed improved motor function.[9] The

investigators suggested that only partial motor improvement was observed in these patients due to sub-optimal coverage of the structure. However, an alternate explanation is that AAV2-hAADC transduces medium spiny neurons when infused into putamen. These cells do not synthesize appreciable amounts of L-DOPA, the substrate for AADC-catalyzed dopamine and serotonin synthesis. Thus, optimal improvement in motor function would not be expected in the absence of exogenous L-DOPA. The investigators did report elevated CSF levels of L-DOPA and presumably the transgenic AADC was able to make use of that.[9] However, the intracellular concentration of L-DOPA in medium spiny neurons in that context would probably be low. In contrast, L-DOPA is produced in the SNpc and VTA, and AADC-deficient patients, in contrast to PD patients, have an intact nigrostriatal pathway.[1] Thus, AAV2-hAADC transduction of SNpc and VTA should result in the replacement of the missing enzyme in the cells that would already make L-DOPA in abundance[22] and would thus be expected to direct dopamine synthesis as efficiently as in normal children. As there is currently no vertebrate animal model of AADC deficiency, we performed this toxicology study in naïve NHP and did not look for efficacy outcomes. However, we have previously demonstrated the functionality of this AAV2-hAADC vector in rats[23] and we also performed an *in vitro* assay that confirmed the increased conversion of L-DOPA to dopamine in cells transduced with the present AAV2-hAADC vector (Supplementary Figure S2).

Our present data demonstrate that this vector can be safely delivered to SNpc and VTA with the FDA-approved SmartFlow cannula specifically designed for clinical application,[13,14] with no appearance of adverse effects for up to 9 months after the procedure. The reliability of the SmartFlow cannula and direct delivery procedure we used is demonstrable in the small standard deviation of Vd/Vi data among the 36 infusions performed in this study. Reliable delivery is critical when targeting brain regions like the mid-brain, that contain many brain nuclei, in order to minimize off-target distribution and potential adverse effects. All animals receiving AAV2-hAADC showed good coverage of the target structures. Although MR tracer images could not be directly matched with AADC staining due to endogenous AADC expression, enhanced hAADC expression was detected in the same mid-brain regions as the MR tracer, including the SNpr which does not normally express this enzyme. Furthermore, AAV2-hAADC-treated animals' striata showed a wide network of strongly AADC-ir fibers in comparison to the significantly fainter endogenous AADC staining in control animals. These data confirmed the cytoplasmic distribution of the transgenic protein in nigral axonal projections to striatum. In some cases, cannula placement was slightly lateral and the infusion did not properly reach VTA, resulting in a lack of transduction of this area. This would explain the lack of AADC-ir fibers in the nucleus accumbens. One aim of this study was to reveal exactly this type of anomaly. Therefore, our planned clinical trial will include two infusion sites: one in the SN and another in the VTA. The corresponding structures (*i.e.*, SNpc and VTA) in human children are ~10-fold greater in volume than in NHP.[24] Thus, allowing for structural differences as well as clinical experience from our AAV2-hAADC studies in PD and the Taiwanese AADC deficiency, we estimate that a volume of 50 µl in the SNpc would be optimal and the corresponding volume to be delivered in AADC-deficient children (on each side). Interestingly, one of the pilot animals received almost 50 µl on the right SNpc and no behavioral or histological adverse effects were reported up to 1 month after the infusion, indicating that higher volumes than those in our toxicology study are likely to be safe.

Transduction of SNpc and VTA with this approach yielded broad expression of transgenic AADC in the nigro-striatum. There were no behavioral symptoms reported in any of the animals, control or AAV2-hAADC-treated, for either 1-, 3-, or 9-month survival times. Accordingly, no histological indications of parenchymal injury due to cannula insertion, other than the expected gliosis and macrophages, were found despite two cannula insertions occurring close to each other in the mid-brain of every animal. An independent histopathology report found that some perivascular infiltrates were associated with AAV2-hAADC infusion. However, such infiltrates were also present in control animals. This type of response to the surgical injury seems to be caused by cannula insertion. In our experience, it resolves over time and has no persistent associated pathology.[18]

Assessment of vector distribution revealed that systemic exposure occurred during or immediately after AAV2-hAADC high vector dose delivery, but vector DNA was cleared from blood by the time of necropsy. Also, evaluation of CSF samples at baseline and necropsy showed no significant changes in dopamine, serotonin and their metabolites after AADC gene transfer indicating that AADC activity was likely localized in areas of observed AADC expression within the brain. Similarly, serum and CSF levels of AADC protein were not generally affected by AAV2-hAADC delivery. Taken together, all these data demonstrate the safety of the surgical procedure and long-term expression of AAV2-hAADC in the mid-brain.

A recent follow-up imaging study on PD patients from the AAV2-hAADC phase 1 trial, demonstrated stable AADC expression by positron emission tomography with [^{18}F]fluoro-L-metatyrosine tracer and continued safety over 4 years after vector delivery.[21] Accordingly, in this study, AAV2-hAADC delivery in the mid-brain and wide AADC expression in the striatum for up to 9 months after delivery was accompanied by no severe adverse effects and was well tolerated for up to 9 months.

Mutations in the *DDC* gene that cause AADC deficiency pathology cause a profound deficit in AADC enzyme in the brain (and peripheral organs), not only in the SNpc and VTA but also in the raphe nuclei that synthesizes serotonin. Thus, disease symptoms include not only motor deficits but also mental retardation and autonomic dysfunction.[3,25] The approach presented in this study aims to alleviate the motor symptoms in AADC deficiency patients, but they may also further benefit from AAV2-hAADC delivery into the raphe nuclei. Since subsequent treatments in this brain region could be performed in patients who would have already received a primary SN/VTA infusion, the potential impact of anti-AAV2 and anti-hAADC antibodies was investigated. Although no significant antibody titer was found against AADC for any of the experimental groups, production of anti-AAV2 neutralizing antibodies was dose-dependent with antibodies detected only in the high-dose animals. Neutralizing anti-AAV2 antibodies are not anticipated to cause any adverse effects below a titer of 1:1,200,[26] but could inhibit subsequent AAV2-mediated gene transfer if higher titers were generated. This potential problem could be overcome perhaps by using a different AAV serotype to carry the hAADC transgene, although cross-reactivity of anti-AAV2 antibodies could still be an issue.[27] Another potential concern often voiced by investigators in the field of recessive genetic diseases is the idea that introducing a protein never seen by the immune system might trigger immunity against the transgene. However, this consideration, perhaps concerning in other types of therapies, is considered unlikely in this situation because AAV2 is neuron-specific when infused into the brain and, as we have shown, is highly contained within target structures when our high-precision system is employed.

Altogether, this study demonstrates the long-term safety and tolerability of a single-dose administration of AAV2-hAADC into the

mid-brain of NHP by real-time image-guided infusion. The data are supportive of clinical evaluation of this gene therapy in AADC deficiency disease.

MATERIALS AND METHODS

Animals

Eighteen adult Cynomolgus monkeys *(Macaca fascicularis*, 3–7 kg, 9 males, 9 females) were included in this study. Individual animals were assigned to 2 experiments: an initial pilot study to examine vector distribution, dose-ranging and initial safety after delivery into the mid-brain ($N = 2$) and a pivotal safety and toxicology study, performed in accord with Good Laboratory Practice standards, with a maximum in-life duration of 9 months after vector administration (Control group (vehicle, $N = 4$), AAV2-hAADC low-dose group ($N = 6$) and high-dose group ($N = 6$)). In the latter experiment, animals were assigned by random order selection; additional selection and distribution of animals across groups was made to obtain groups with comparable mean body weights. The animals received simultaneous bilateral infusion of either vehicle or AAV2-hAADC (low or high dose) into the SNpc and VTA and were monitored for either 1, 3, or 9 months after infusion (Table 1).

In-life observations

Cage-side observations were performed twice daily throughout the study to evaluate general health, appearance, and appetite of all animals. Animals were weighed prior to surgery, weekly for the first 4 weeks after surgery, and biweekly thereafter until the conclusion of the study. Also, a battery of neurobehavioral evaluations, designed to assess central/peripheral nervous system status, was conducted by an examiner blinded to treatment group on all animals at baseline and prior to necropsy. Pilot animals were housed at the Laboratory Animal Research Center in the University of California San Francisco (San Francisco, CA) and the pivotal safety and toxicology study was performed at Inc. (VBS, West Sacramento, CA). Use of animals for these studies was approved by the Institutional Animal Care and Use Committee at University of California San Francisco and the VBS Animal Care and Use Committee, respectively, and in accordance to the National Institutes of Health guidelines.

Vector production and preparation

Both control and test articles were manufactured at Children's Hospital of Philadelphia (Philadelphia, PA). The human AADC cDNA was cloned into an AAV2 shuttle plasmid, and a recombinant AAV2 containing hAADC under the control of the cytomegalovirus promoter was manufactured by the AAV Clinical Vector Core at Children's Hospital of Philadelphia via a Good Manufacturing Practice process-comparable lot as previously described.[28] Briefly, AAV2-hAADC was generated by helper virus free transfection of HEK293 cells, and the vector purified from harvested cells and medium after cell lysis and clarification by combined ion exchange chromatography and isopycnic CsCl gradient centrifugation, and then diafiltered by tangential flow filtration against 180 mmol/l sodium chloride, 10 mmol/l sodium phosphate, pH 7.3 and concentrated to a final concentration of ~8.3×10^{12} vector genomes (vg)/ml. After TFF, Pluronic F68 was added to a final concentration of 0.001%. The test article was thawed and diluted with excipient (180 mmol/l sodium chloride, 10 mmol/l sodium phosphate, 0.001% v/v Pluronic F68, pH 7.3) to achieve the designated concentrations immediately prior to dosing (low dose: 8.3×10^{11} vg/ml; high dose: 8.3×10^{12} vg/ml). Gadoteridol (ProHance, Bracco Diagnostics, Princeton, NJ), a magnetic resonance (MR) contrast agent, was added to the dosing solutions at a concentration of 2 mmol/l (1:250 dilution of ProHance) to enhance visibility of the infusion on MR. Vector functionality was assayed by measuring the conversion of L-DOPA to dopamine *in vitro* (Supplementary Materials and Methods).

Surgical procedure and image-guided delivery

Animals were sedated with an intramuscular injection of ketamine (10 mg/kg) and medetomidine (0.015 mg/kg). A tracheal intubation procedure was performed and the animals were placed on inhaled isoflurane (1–4%).

Each NHP was placed supine in a MRI-compatible stereotactic frame. After craniectomy, an adjustable MRI-compatible cannula trajectory guide device was secured to the skull over each hemisphere. After placement of the cannula guides, the intubated animal was moved into a 1.5T GE MRI scanner. High-resolution anatomical MR scans were performed for target identification and surgical planning.

Once the target was selected and cannula guides were aligned to the desired trajectory, SmartFlow cannulae (MRI Interventions, Irvine, CA) custom-designed for pressurized infusions[29,30] were used to infuse the vector. Each SmartFlow cannula was attached to a 1-ml syringe mounted onto a MRI-compatible infusion pump (Medfusion 3500 syringe pump, Medfusion, St Paul, MN). Briefly, pumps were started at 1 µl/minute and, after visualizing fluid flow from the cannula tip when held at the height of the NHP head, the cannula was inserted through the cannula-guide and into the brain to the target depth. In the pilot study, one animal received 26 µl on left side and 46 µl on the right, and the second animal received 30 µl on the left and 28 µl on the right. The infusion rate was stepped up from 1 to 2 µl/minute based on real-time MR images of the gadolinium signal during the infusion. In the IND-enabling toxicology study, all animals received a uniform volume of 30 µl to each side (60 µl total) at an initial rate of 1 µl/minute for 10 minute followed by a rate of 2 µl/minute for 10 minute. Immediately after completion of the MRI-guided infusions, each animal was returned to surgery where the cannula guides were removed and incisions sutured. Then, animals were moved to their home-cage and monitored for full recovery from anesthesia.

MR imaging data analysis

Prior to cannula insertion, MR images were acquired via previously established methods to plan and determine precise placement of the infusion- and guide-cannula within the SNpc. Briefly, T1-weighted images of the primate brain were acquired on a 1.5T Signa HDxt scanner (GE Medical Systems, Waukesha, WI) with two 5-inch surface coils. Prior to insertion of the SmartFlow cannulae, baseline three-dimensional spoiled gradient echo (3D SPGR) images were taken: repetition time (TR)/echo time (TE)/flip angle = 3.9 ms/1.54 ms/15°, number of excitations (NEX) = 4, matrix = 256×192, field of view (FOV) = 16×12 cm, slice thickness = 1 mm. Once the catheters were inserted and the infusion commenced, SPGR scans were acquired consecutively throughout the infusion procedure (acquisition time was ~2.5 minute per sequence) to monitor distribution from the cannula tip. Distribution volumes (Vd) of gadolinium were measured on MR images with Osirix (Geneva, Switzerland), an open source DICOM reader and imaging workstation. Software was written and applied as an Osirix plug-in to auto-segment each infusion on individual MRI slices from which a total distribution volume was calculated.[31] The ratio (Vd/Vi) between volume of distribution (Vd) and the infusion volume (Vi) was calculated for each hemisphere in all animals and data presented as mean ± SD for each hemisphere. The gadolinium-enhanced regions on the images were also visualized using iPlan 3.0.3 workstation (Brainlab; Munich, Germany). The workflow used standard semi-automatic segmentation (iPlan Smartbrush) to generate three-dimensional reconstructions of the infusate distribution. A blinded intraoperative correlation validated the reconstruction results of enhanced regions and cannula trajectory for each group assignment.

Histopathological analysis

Animals were euthanized either 1, 3, or 9 months after intracranial dosing procedures (Table 1) by transcardial perfusion with either PBS-heparin and 4% paraformaldehyde (PFA)/PBS (pilot study) or PBS-heparin alone (toxicology study). Gross necropsy and tissue examinations were performed by a veterinary pathologist for both studies. For the pilot study, brains and spinal cord samples were collected and postfixed in 4% PFA overnight. Brain-blocks were then cut into 40-µm sections in a sliding microtome and cryopreserved in anti-freeze solution until further analysis. For the IND-enabling toxicology study, the brain and spinal cord were blocked and immersion-fixed in 4% PFA and samples of major peripheral organs were immersion-fixed in 10% formalin. Brain-blocks containing either SNpc/VTA (infusion site), basal ganglia (striatum, globus pallidus, subthalamic nucleus), thalamus, brainstem, cortex, spinal cord and peripheral organs samples were subjected to histopathology analysis by an independent pathology group (Seventh Wave Laboratories, LLC) blinded to treatment groups.

Histological analysis of transgene expression

To assess transgene expression, brain sections from both studies were processed for double immunohistochemistry (IHC) with antibodies to detect AADC protein (endogenous and transgenic) and tyrosine hydroxylase (TH), the latter a counterstain to identify striatum, SNpc and VTA.

Briefly, sections were first de-paraffinized, if needed, in Clear Rite 3 (Thermo Scientific, Waltham, MA) and graded alcohols, rehydrated and treated for antigen-retrieval in Diva Decloaker solution (Biocare Medical, Concord, CA) in a decloaking chamber. Sections were washed

in Tris-buffered saline (TBS) followed by treatment with 1.5% v/v H_2O_2 in TBS to block endogenous peroxidase. Sections were then incubated in Sniper blocking solution (Biocare Medical) followed by incubation overnight at 4 °C with primary antibodies (rabbit polyclonal anti-DDC, 1:1,000, cat. AB136 and anti-TH, 1:5,000, cat. MAB 318, Millipore, Billerica, MA). Sections were rinsed in TBS and incubated in Mach 2 Rabbit HRP Polymer (Biocare Medical) and Mouse AP Polymer (Biocare Medical) for 1 hour, followed by several washes and colorimetric development with Vector Blue (Vector Blue Alkaline Phosphatase substrate kit, cat. SK-5300; Burlingame, CA) and either Vector NovaRED (Vector NovaRED Peroxidase substrate kit, cat. SK-4800; Burlingame, CA) or 3,3′-diaminobenzidine (DAB Peroxidase substrate kit, cat. SK-4100; Burlingame, CA). Immunostained sections were dehydrated in graded alcohols and or Clear Rite 3 and cover-slipped with a toluene-based mounting media (Shandon-Mount, Thermo Scientific). For hematoxylin and eosin (H&E) staining, sections were de-paraffinized if needed, rehydrated and stained with hematoxylin (Buffalo Grove, IL) for 3 minute, washed with water and then differentiated in 0.5% v/v acetic acid/70% alcohol followed by staining in bluing solution (Thermo Scientific). After incubation in eosin (Buffalo Grove, IL), the sections were dehydrated in alcohol and xylene, and cover-slipped.

Transgene expression analysis was performed for both the pilot and toxicological studies. For the pilot study sections, the SNpc/VTA and striatum were double-stained to assess vector distribution and transgenic protein transport to neuronal terminals. For the toxicological study, transgenic AADC expression was analyzed as follows. For AADC expression in the striatum, coronal sections ($N = 4$ per animal) containing precommissural, commissural and postcommissural striatum were analyzed for AADC expression in nigrostriatal projections. Endogenous AADC immunoreactivity (ir) observed in the striatum of control animals was significantly lower than that from transgenic AADC expression in AAV2-hAADC treated animals, thereby permitting reliable detection of transgenic hAADC expression in striatum. AADC-ir in control group sections was used as a reference for the assessment of the expression of hAADC in treated animals (low-dose and high-dose groups). In order to evaluate transgenic hAADC protein distribution, doubly stained striatal sections were rated for the presence of fibers expressing hAADC in both caudate and putamen (−: absent (endogenous AADC staining); +: low intensity/sparse fiber staining; ++: intermediate intensity/many positive fibers; +++: high intensity/dense fiber staining).

For AADC expression in structures outside the infusion target, coronal sections ($N = 4$ per animal) containing basal ganglia and other nuclei were analyzed for AADC expression. AADC-ir in control group sections was used as the reference for the assessment of the off-target expression of transgenic AADC in AAV2-hAADC treated animals (low-dose and high-dose groups). Sections were checked for transgenic hAADC expression in basal ganglia (other than striatum), brainstem and spinal cord. High levels of endogenous AADC protein did not permit assessment of transgenic hAADC expression in VTA and SNpc. All histological analysis of all sections was performed by observers blind to treatment group identities.

Blood and cerebrospinal fluid sampling

Serum samples were collected for hematology, clinical pathology, AADC levels and vector distribution at baseline, 4 hours, 24 hours, 15 days, 1, 3, 6, and 9 months from the toxicology study animals only. Serum samples for anti-AAV2 and anti-AADC antibody detection were collected at baseline, day 15, and at necropsy. Whole blood samples (0.5 ml) were collected in EDTA tubes and stored at 4 C until further processing. Similarly, blood for serum samples from the animals in the toxicology study were collected in serum separator tubes with clot activator, allowed to clot for 30 minute and spun for 15 minute at 3,000 rpm. Serum was transferred to tubes with no additive and frozen until further use.

In the same animals, CSF was collected prior to parenchymal dosing procedures and immediately prior to necropsy for monoamines and AADC protein assessment. All CSF samples were collected in sterile 1.5 ml centrifuge tubes, except those for vector biodistribution that were collected in DNase- and RNase-free sterile 1.5 ml centrifuge tubes. Both blood serum and CSF samples were collected for assay of anti-AAV2 and anti-AADC antibodies.

Monoamine level assessment (HPLC) in CSF

Monoamine levels were measured in CSF at baseline and at necropsy for toxicological study animals. Ice-cold 7 mol/l perchloric acid (1.5 µl) was added to each CSF sample (100 µl). Samples were then vortexed and centrifuged at 14,000 rpm for 15 minute at 4 °C. The supernatant was transferred to a 1.5 ml centrifuge tube and centrifuged again as above. The supernatant was then filtered through a 0.20 µm membrane syringe Whatman filter (Sigma Aldrich, St Louis, MO) and injected onto high-performance liquid chromatography (HPLC) system coupled to electrochemical detection (ECD, CoulArray 5600A, ESA, Chelmsford, MA) for determination of dopamine, DOPAC, HVA, serotonin and 5-HIAA.

Supernatant (30 µl) was injected onto the HPLC-ECD system as previously described.[23] In parallel with CSF samples, a series of standard solutions (Sigma Aldrich) with known concentrations of these catecholamines (1,000 ng/ml, 100 ng/ml and 20 ng/ml) were also chromatographed. Dopamine, DOPAC, HVA, serotonin and 5-HIAA in CSF samples were identified by retention times of standards and quantified by measuring the area under the peaks with CoulArray Data Station 3.00 software (ESA, Chelmsford, MA). The limit of quantification was set at 10 ng/ml. Concentrations (ng/ml) in CSF samples were reported by comparison with the standard curves.

AADC protein levels and AAV2-hAADC biodistribution in serum and CSF

Serum samples taken at baseline, 4 hours, 24 hours, 15 days, 1, 3, 6, and 9 months after infusion were analyzed for AADC levels and biodistribution. CSF was collected only at baseline and at necropsy for these analyses.

Quantification of AADC protein in serum and CSF samples was performed by sandwich ELISA assay as previously described. A commercially available kit "Human DOPA Decarboxylase/DDC ELISA Pair Set" (Sino Biological Inc., Beijing, China) was used for this assay. ELISA was performed according to the manufacturer's protocol. Absorbance (TMB substrate) at 450 nm was proportionate to the amount of AADC present in the sample. The minimum detectable concentration of AADC in the assay was determined to be 62.5 pg/ml.

Quantitative polymerase chain reaction (Q-PCR) of AAV2-hAADC vector DNA in serum and CSF samples at baseline and necropsy was performed with a fluorogenic 5′-nuclease assay (TaqMan, Applied Biosystems, Foster City, CA) on an Applied Biosystems ViiA 7 Real-Time PCR System (Applied Biosystems, Foster City, CA) as previously described.[32] Real-time Q-PCR was standardized with plasmid DNA containing the vector insert (pAAV-hAADC2; Lot# 3321850). The plasmid was linearized with EcoRV, purified, quantified by ultraviolet absorbance, and diluted in Q-PCR dilution buffer to generate 7 standards ranging from 10 to 1×10^6 copies/reaction. Each standard was run in 3 replicate 20-µl reactions in a 384-well optical plate. Genomic DNA was isolated from serum and CSF by means of QIAamp DNA Blood Mini Kit (Qiage, Valencia, CA). To increase the yield of DNA isolation from cell-free serum and CSF samples, per manufacturer's recommendation, carrier DNA (salmon sperm DNA) was added to Buffer AL (5 µg per 200 µl). A sentinel control sample (salmon sperm DNA alone) was also isolated at the same time to monitor for contamination. Genomic DNA isolated from each sample (200 µl of serum or CSF) was assayed for AAV2-hAADC. Of the total 50-µl DNA elute, 5 µl was assayed for AAV2-hAADC (each reaction). In addition, three random samples were spiked with 100 copies of the vector standard and assayed to monitor the PCR reaction efficiency. Samples with low reaction efficiency (<75%) were presumed to contain PCR inhibitors that affected sensitivity. In the presence of AAV2-hAADC DNA, the AAV2-hAADC-specific primers amplify a 70-base pair region of exon 7 and 8 of the AAV2-hAADC target (Life Technologies, Foster City, CA). Spanning an intron absent from the vector sequence minimizes amplification of genomic DNA. During the extension step at 60 °C, the AAV2-hAADC-specific probe is incorporated into the amplicon and releases the attached 6-carboxyfluorescein. The amount of fluorescence generated is proportional to the number of AAV2-hAADC amplicons generated during the run, and is related to the initial amount of AAV2-hAADC template present in each sample. Human AADC cDNA copies were calculated by multiplying the copies per well by 2, assuming that 1 copy of double-stranded plasmid DNA is equivalent to two single-stranded vector genomes. Upper and lower limits of quantitation were selected as the highest and lowest points on the standard curve (10 - 10^6 copies and 10 copies of AAV2-hAADC per reaction, respectively).

Anti-AAV2 and anti-AADC neutralizing antibody titers

To screen for AAV2 neutralizing activity in NHP serum, samples were collected prior to surgery (baseline) and at necropsy. The neutralizing titer was determined *in vitro* in a cell-based assay. Serum samples were serially diluted (lowest dilution 1:25) with DMEM culture medium containing 2% FBS and incubated with AAV2-green fluorescent protein (GFP), 4×10^8 vg at 37 °C. One hour after mixing the vector and serum samples, 50% of the mixture of serum/vector (20 µl) was added (in triplicate) to HT1080 cells seeded the previous day at 20,000 cells per well (100 µl) of 96-well plates

(clear bottom, black walls). The final multiplicity of infection for each well was 10,000. In parallel, the same amount of vector but without NHP serum was added to cells for vector control standard. Blank (negative control) determinations omitted the vector. The cells were grown for 2 days and, after one wash in PBS, the level of GFP expression (fluorescence) was measured in a FL-800 Biotek plate reader (Biotek, Winooski, VT) with a green filter (488 nm). After subtracting the background (values of blank controls with no virus added), the mean values from each triplicate were calculated and compared with the positive control/standard (AAV2 with no NHP serum added). AAV2 neutralizing antibody titer is the highest dilution of serum that results in 50% reduction in fluorescence when compared with untreated vector.

Antibodies against AADC protein were detected in NHP serum by incubating serial dilutions of serum (1:2, 1:8, 1:32, 1:128, 1:512, 1:2,048, and 1:8,192) with 60 ng recombinant human AADC protein (R&D Systems, Minneapolis, MN) per well immobilized on wet nitrocellulose in a Bio-Dot Microfiltration apparatus (Bio-Rad, Hercules, CA) following the manufacturer's protocol. Serum samples were collected at baseline, at various in-life intervals (1, 3, and 9 months), and at necropsy. Horseradish peroxidase-conjugated goat anti-monkey IgG (Fitzgerald, Acton, MA) was used as a secondary antibody (1:5,000 dilution) and color development of enzyme-conjugated antibodies was performed by Immun-Blot Opti-4CN Colorimetric kit (Bio-Rad). Once dry, membranes were digitized and generated images were analyzed with ImageJ software.[33] The upper and lower limits of intensity for this assay were standardized to establish the dynamic range for ratio calculation as ≤20,000 to ≥5,000 arbitrary units, respectively.

CONFLICT OF INTEREST

The authors declare no conflict of interest.

ACKNOWLEDGMENTS

The authors thank Valley Biosystems and Seventh Wave Laboratories for performing in-life evaluations and histopathology report, respectively. This work was supported by NIH grant X01 NS073514-01 to KSB, Pediatric Neurotransmitter Deficiency Foundation and AADC Trust Foundation, UK.

REFERENCES

1. Lee, HF, Tsai, CR, Chi, CS, Chang, TM and Lee, HJ (2009). Aromatic L-amino acid decarboxylase deficiency in Taiwan. *Eur J Paediatr Neurol* **13**: 135–140.
2. Manegold, C, Hoffmann, GF, Degen, I, Ikonomidou, H, Knust, A, Laass, MW *et al*. (2009). Aromatic L-amino acid decarboxylase deficiency: clinical features, drug therapy and follow-up. *J Inherit Metab Dis* **32**: 371–380.
3. Hyland, K and Clayton, PT (1990). Aromatic amino acid decarboxylase deficiency in twins. *J Inherit Metab Dis* **13**: 301–304.
4. Brun, L, Ngu, LH, Keng, WT, Ch'ng, GS, Choy, YS, Hwu, WL *et al*. (2010). Clinical and biochemical features of aromatic L-amino acid decarboxylase deficiency. *Neurology* **75**: 64–71.
5. Hoffmann, GF, Assmann, B, Bräutigam, C, Dionisi-Vici, C, Häussler, M, de Klerk, JB *et al*. (2003). Tyrosine hydroxylase deficiency causes progressive encephalopathy and dopa-nonresponsive dystonia. *Ann Neurol* **54 (suppl. 6)**: S56–S65.
6. Yahr, MD, Duvoisin, RC, Schear, MJ, Barrett, RE and Hoehn, MM (1969). Treatment of parkinsonism with levodopa. *Arch Neurol* **21**: 343–354.
7. Christine, CW, Starr, PA, Larson, PS, Eberling, JL, Jagust, WJ, Hawkins, RA *et al*. (2009). Safety and tolerability of putaminal AADC gene therapy for Parkinson disease. *Neurology* **73**: 1662–1669.
8. Muramatsu, S, Fujimoto, K, Kato, S, Mizukami, H, Asari, S, Ikeguchi, K *et al*. (2010). A phase I study of aromatic L-amino acid decarboxylase gene therapy for Parkinson's disease. *Mol Ther* **18**: 1731–1735.
9. Hwu, WL, Muramatsu, S, Tseng, SH, Tzen, KY, Lee, NC, Chien, YH *et al*. (2012). Gene therapy for aromatic L-amino acid decarboxylase deficiency. *Sci Transl Med* **4**: 134ra61.
10. Johnston, LC, Eberling, J, Pivirotto, P, Hadaczek, P, Federoff, HJ, Forsayeth, J *et al*. (2009). Clinically relevant effects of convection-enhanced delivery of AAV2-GDNF on the dopaminergic nigrostriatal pathway in aged rhesus monkeys. *Hum Gene Ther* **20**: 497–510.
11. Kells, AP, Forsayeth, J and Bankiewicz, KS (2012). Glial-derived neurotrophic factor gene transfer for Parkinson's disease: anterograde distribution of AAV2 vectors in the primate brain. *Neurobiol Dis* **48**: 228–235.
12. Ciesielska, A, Mittermeyer, G, Hadaczek, P, Kells, AP, Forsayeth, J and Bankiewicz, KS (2011). Anterograde axonal transport of AAV2-GDNF in rat basal ganglia. *Mol Ther* **19**: 922–927.
13. Richardson, RM, Gimenez, F, Salegio, EA, Su, X, Bringas, J, Berger, MS *et al*. (2011). T2 imaging in monitoring of intraparenchymal real-time convection-enhanced delivery. *Neurosurgery* **69**: 154–63; discussion 163.
14. Richardson, RM, Kells, AP, Martin, AJ, Larson, PS, Starr, PA, Piferi, PG *et al*. (2011). Novel platform for MRI-guided convection-enhanced delivery of therapeutics: preclinical validation in nonhuman primate brain. *Stereotact Funct Neurosurg* **89**: 141–151.
15. San Sebastian, W, Richardson, RM, Kells, AP, Lamarre, C, Bringas, J, Pivirotto, P *et al*. (2012). Safety and tolerability of magnetic resonance imaging-guided convection-enhanced delivery of AAV2-hAADC with a novel delivery platform in nonhuman primate striatum. *Hum Gene Ther* **23**: 210–217.
16. Bankiewicz, KS, Forsayeth, J, Eberling, JL, Sanchez-Pernaute, R, Pivirotto, P, Bringas, J *et al*. (2006). Long-term clinical improvement in MPTP-lesioned primates after gene therapy with AAV-hAADC. *Mol Ther* **14**: 564–570.
17. Forsayeth, JR, Eberling, JL, Sanftner, LM, Zhen, Z, Pivirotto, P, Bringas, J *et al*. (2006). A dose-ranging study of AAV-hAADC therapy in Parkinsonian monkeys. *Mol Ther* **14**: 571–577.
18. Hadaczek, P, Eberling, JL, Pivirotto, P, Bringas, J, Forsayeth, J and Bankiewicz, KS (2010). Eight years of clinical improvement in MPTP-lesioned primates after gene therapy with AAV2-hAADC. *Mol Ther* **18**: 1458–1461.
19. Daadi, MM, Pivirotto, P, Bringas, J, Cunningham, J, Forsayeth, J, Eberling, J *et al*. (2006). Distribution of AAV2-hAADC-transduced cells after 3 years in Parkinsonian monkeys. *Neuroreport* **17**: 201–204.
20. Eberling, JL, Jagust, WJ, Christine, CW, Starr, P, Larson, P, Bankiewicz, KS *et al*. (2008). Results from a phase I safety trial of hAADC gene therapy for Parkinson disease. *Neurology* **70**: 1980–1983.
21. Mittermeyer, G, Christine, CW, Rosenbluth, KH, Baker, SL, Starr, P, Larson, P *et al*. (2012). Long-term evaluation of a phase 1 study of AADC gene therapy for Parkinson's disease. *Hum Gene Ther* **23**: 377–381.
22. Dahlstroem, A and Fuxe, K (1964). Evidence for the existence of monoamine-containing neurons in the central nervous system. I. Demonstration of monoamines in the cell bodies of brain stem neurons. *Acta Physiol Scand Suppl* **232**: 231–255.
23. Ciesielska, A, Hadaczek, P, Mittermeyer, G, Zhou, S, Wright, JF, Bankiewicz, KS *et al*. (2013). Cerebral infusion of AAV9 vector-encoding non-self proteins can elicit cell-mediated immune responses. *Mol Ther* **21**: 158–166.
24. Yin, D, Valles, FE, Fiandaca, MS, Forsayeth, J, Larson, P, Starr, P *et al*. (2009). Striatal volume differences between non-human and human primates. *J Neurosci Methods* **176**: 200–205.
25. Hyland, K, Surtees, RA, Rodeck, C and Clayton, PT (1992). Aromatic L-amino acid decarboxylase deficiency: clinical features, diagnosis, and treatment of a new inborn error of neurotransmitter amine synthesis. *Neurology* **42**: 1980–1988.
26. Sanftner, LM, Suzuki, BM, Doroudchi, MM, Feng, L, McClelland, A, Forsayeth, JR *et al*. (2004). Striatal delivery of rAAV-hAADC to rats with preexisting immunity to AAV. *Mol Ther* **9**: 403–409.
27. Calcedo, R, Vandenberghe, LH, Gao, G, Lin, J and Wilson, JM (2009). Worldwide epidemiology of neutralizing antibodies to adeno-associated viruses. *J Infect Dis* **199**: 381–390.
28. Wright, JF, Wellman, J and High, KA (2010). Manufacturing and regulatory strategies for clinical AAV2-hRPE65. *Curr Gene Ther* **10**: 341–349.
29. Krauze, MT, Saito, R, Noble, C, Tamas, M, Bringas, J, Park, JW *et al*. (2005). Reflux-free cannula for convection-enhanced high-speed delivery of therapeutic agents. *J Neurosurg* **103**: 923–929.
30. Fiandaca, MS, Forsayeth, JR, Dickinson, PJ and Bankiewicz, KS (2008). Image-guided convection-enhanced delivery platform in the treatment of neurological diseases. *Neurotherapeutics* **5**: 123–127.
31. Rosenbluth, KH, Gimenez, F, Kells, AP, Salegio, EA, Mittermeyer, GM, Modera, K *et al*. (2013). Automated segmentation tool for brain infusions. *PLoS ONE* **8**: e64452.
32. Cunningham, J, Pivirotto, P, Bringas, J, Suzuki, B, Vijay, S, Sanftner, L *et al*. (2008). Biodistribution of adeno-associated virus type-2 in nonhuman primates after convection-enhanced delivery to brain. *Mol Ther* **16**: 1267–1275.
33. Schneider, CA, Rasband, WS and Eliceiri, KW (2012). NIH Image to ImageJ: 25 years of image analysis. *Nat Methods* **9**: 671–675.

Supplementary Information accompanies this paper on the *Molecular Therapy—Methods & Clinical Development* website (http://www.nature.com/mtm)